1975

MODELING OF ATMOSPHERIC TRANSPORT AND FUMIGATION AT SHORELINE SITES

R. N. MERONEY and J. E. CERMAK

Fluid Dynamics and Diffusion Laboratory, Civil Engineering Dept., Colorado State University, Fort Collins, Colo., U.S.A.

and

B. T. YANG

Stone and Webster Engineering Corporation, Boston, Mass., U.S.A.

(Received in final form 27 March, 1975)

Abstract. Plumes initially exhausted into stable air over water disperse slowly; yet after crossing a coastline and travelling inland for a sufficient distance, the plumes interact with thermals rising from the land and may be brought rapidly to the ground. Model studies of a typical power plant sited along a lake shoreline were made to determine mixing-layer growth over the land and fumigation potential of elevated releases. An atmospheric boundary-layer wind tunnel simulated water and land temperature differences and an initially ground-based inversion approach flow.

Nomenclature

C_p	Specific heat capacity
D_s	Stack diameter
Fr	Stack gas Froude Number $(\varrho_a V_a^2/\Delta\gamma D_s)$
Fr_δ	Upstream flow Froude Number $(V_a^2/g\delta)$
g	Gravitational acceleration
H	Mixed-layer thickness
HR	Heating ratio $(\Delta T/\Delta\theta)$
h_s	Stack height
Δh_s	Added effective stack height
k	von Kármán Constant
K	Constant
L	Scale ratio h_s/D_s
L_x	Length scale, horizontal
L_z	Length scale, vertical
L_{MO}	Monin-Obukhov scale $(-\varrho C_p T U^{*3}/kgq)$
P	Pressure
q	Heat flux
R	Velocity ratio (V_s/V_a)
Ri_B	Bulk Richardson Number $(g(\Delta\theta/T)\,(\delta/V_a^2)$
T	Absolute temperature
ΔT	Sea-land temperature difference
$\Delta\theta$	Vertical temperature difference over reference height L_z
U_*	Friction velocity
V_a	Ambient wind velocity at reference height L_z
V_s	Stack velocity
x	Distance
z_0	Roughness height
δ	Length scale for height
ϱ	Density
$\Delta\gamma$	Specific weight
χ	Concentration

Boundary-Layer Meteorology **9** (1975) 69–90.

1. Introduction

When air blows over a cold water surface, the lower layers of the atmosphere are cooled and an inversion develops to a depth of from 30 to 300 m. During an onshore wind this stable marine layer is heated from below after crossing the coastline, creating a superadiabatic lapse rate in the lower levels while retaining a stable condition above. With increased distance from the shoreline, the heated region, or mixed layer, grows vertically until the original stable layer is destroyed. If a tall stack associated with a power plant that is located near the shoreline discharges into the elevated stable layer, the plume initially disperses slowly as it moves downwind. At some point inland, the mixing layer extends upward to the plume level. At this point, material in the plume mixes rapidly downward to cause 'fumigation' and high concentrations at ground level (Barrett, 1973; Lyons, 1970; Lyons and Cole, 1971, 1973; Lyons and Olsson, 1973; Collins, 1971; Van der Hoven, 1967).

The determination of the spatial extent of the diffusion transition zone becomes an important aspect of the environmental evaluation of industry, fossil-fuel power plants, and nuclear reactors located at coastlines. In the following sections the properties of thermally modified onshore flows are reviewed, and the heuristic methods utilized to predict fumigation concentrations are considered. Finally an exploratory wind-tunnel experiment incorporating the influence of land-water temperature differences is presented.

2. Properties of Onshore Flow Systems

2.1. Observational evidence

The sea-breeze circulation consists of a landward current near the Earth's surface and a much weaker but deeper return flow aloft about two orders of magnitude smaller. The horizontal scale of the circulation is about 30 to 50 km from the seashore landward, but it varies with land-sea temperature contrasts, and the prevailing synoptic situation. Magnitude of the horizontal velocity is around 10–20 m s^{-1}, and that of the vertical component is 10–20 cm s^{-1} (Fisher, 1960). Humphreys (1964, pp. 157–159) estimated the scale of a sea breeze by using a simple model assuming hydrostatic equilibrium and a constant temperature distribution. He predicted a horizontal scale of about 50 km and a vertical scale of around 300 m – somewhat smaller than observed. The scale of a sea breeze is determined by many factors, such as temperature contrast over the sea and the land, stability conditions in the air, surface roughness of the sea and the land, insolation, and cloud cover. Consequently, the magnitude of the velocities is also a function of the above factors. A land breeze has a smaller scale than a sea breeze. It is weaker over the sea because of smaller temperature differences during the night and the dissipation of energy over the land's rougher surface.

Moroz (1967) observed a lake breeze at a site on the eastern shore of Lake Michigan. The depth of onshore flow in a fully developed lake breeze at the lake shoreline was about 750 m, and horizontal onshore velocities exceeding 7 m s^{-1} were observed. The region of onshore flow extended 25 to 30 km inland but did not reach 53 km for any of the cases observed.

Most recently Lyons (1970) has continued to examine lake breezes on the western and southern shores of Lake Michigan. On two late summer days, inflow depths ranged from 500 to 100 m, with peak inflow velocities of 6–7 m s^{-1}. The breezes penetrated inland more than 40 km. Lyons notes that in the warmer half of the year, the lake-breeze circulation cell developed on almost half of the days, while stable onshore flow associated with synoptic-scale pressure gradients occurred an additional 15% of the time.

2.2. Analytical treatment

A sea-breeze circulation results from a temperature difference between land and sea coupled with a pressure gradient. This may be understood by applying the circulation theorem (for example, Hess, 1959, pp. 244–246). By taking a curl operation over the two-dimensional equation of motion, a vorticity transport equation with a solenoidal term $-\nabla(1/\varrho)\times\nabla P$ is obtained. This forcing function produces a y-direction vorticity component. It always exists unless $-\nabla(1/\varrho)$ and ∇P are parallel. In a sea-breeze situation, pressure distribution is safely assumed to be hydrostatic, which means that ∇P is directed vertically downward. The density over land has a smaller value than that over the sea if height is held constant, because air over land is heated from the surface. Therefore constant density lines decline in the vicinity of a shoreline, which is the physical explanation for the existence of a solenoidal term $-(1/\varrho)\times\nabla P$. Since the governing equations are nonlinear, exact analytical solutions for the sea breeze have not yet been obtained.

Haurwitz (1947) provided one of the earliest efforts in this field by using a circulation theorem. He incorporated a viscosity term in the equations of motion; the term is assumed to be proportional to, and opposite in direction to the local velocity. His conclusion was that the friction term in his model advances the time of maximum intensity of a sea breeze; without the friction term, the maximum occurs when the temperature difference between land and water decreases to zero.

The intensity of a sea breeze is influenced by many factors besides land-water temperature difference. The important roles of gradient wind, topography near the coast, and stability of the atmosphere were discussed by Wexler (1946).

The sea breeze, urban heat island, heated sea island, and heated mountain meteorology are also described in Yamada and Meroney (1971).

The above review suggests that the following physical factors should be included in any simulation of sea breeze circulation development:

(i) Appropriate expressions for eddy diffusivity including the effects of local velocity and temperature.

(ii) Temperature distribution at the surface along the land and the water as governed by the energy balance equations.

(iii) Effect of wind shear.

(iv) The release of latent heat by condensation and evaporation.

(v) The effect of surface roughness change over land and sea.

2.3. Modeling the 'onshore' wind

When vertical motion of plumes takes place in an atmosphere with thermal stratification, additional requirements must be met to achieve similarity of the atmospheric motion. These requirements have been discussed by Cermak (1971), Yamada and Meroney (1971), and SethuRaman and Cermak (1973). Similarity of the stably stratified flow approaching the power plant over a body of water can be achieved by requiring equality of the bulk Richardson number

$$Ri_B = g \frac{\Delta\theta}{T} \frac{\delta}{V_a^2}$$

for the laboratory flow and the atmosphere. In this expression, $\Delta\theta$ is the difference between mean temperature (potential temperature for the atmosphere) at the surface and at the height δ, T is the average temperature over the layer of depth δ and g is the acceleration due to gravitational attraction.

In order to simulate the phenomenon of fumigation resulting from destabilization of the stable lake breeze, similarity must be attained for heat transfer from the warm land surface to the atmosphere. The Monin-Obukhov length scale

$$L_{MO} = \frac{-U_*^3}{(kg/T)\,(q/\varrho C_p)}$$

for similarity of the atmospheric surface layer provides a good gross parameter when combined with the stack height h_s to form a dimensionless ratio h_s/L_{MO}. In this expression, U_* is the shear velocity $(\tau_0/\varrho)^{1/2}$, τ_0 is the surface shear stress, ϱ is the average air density, C_p is the average specific heat for unit mass, q is the surface heat flux and k is the von Kármán constant (0.4). To obtain equality of h_s/L_{MO} for the laboratory flow and the atmosphere, L_{MO} must be 400 times smaller for the laboratory flow than for the atmosphere. This is accomplished by testing at a low velocity V_a of about 0.5 m s^{-1} (this results in a low value for U_*) and heating the laboratory land surface to a high temperature relative to the actual land surface (about 120°C) in order to make q large compared to its value in the atmosphere.

Although one can thus obtain an order-of-magnitude estimate of laboratory simulation conditions, it is expected that the Monin-Obukhov length scale may vary locally as one moves inland from the shoreline. In addition, momentum and heat flux information does not appear to be conveniently available for the field or model cases.

The similarity between the flow-generating mechanisms of sea breezes and flow over 'urban heat islands' suggests alternative parameters. Linear numerical analysis of Olfe and Lee (1971a, b) and experimental and numerical studies by Yamada and Meroney (1971) suggest the intensity of heating by the land surface may be characterized by a heating ratio

$$HR = \frac{(T_{\text{land}} - T_{\text{sea}})_{z_1}}{(T_{z=L_z} - T_{z=z_1})_{\text{over sea}}} \cdot \frac{L_z}{L_x}.$$

Since the vertical-to-horizontal modeling scale is undistorted, the parameter reduces to a single temperature ratio.

A survey was made of available meteorological data which typified 'sea breeze fumigation' situations in the Great Lakes area (Lyons and Cole, 1971, 1973; Lyons, 1970; and Lyons and Olsson, 1973). Only two of four experimental realizations appeared complete enough to estimate the required parameters Ri_B and HR. Table I summarizes the field conditions considered and the resulting range of parameters typical of fumigation. It would appear that laboratory values to examine are:

$$(HR)_p = 1.3 \sim 1.9$$
$$(\mathrm{Ri}_{\mathrm{Bulk}})_p = 1.25 \sim 1.5 \quad \text{at} \quad L_z = 120\ \mathrm{m}.$$

Laboratory conditions were chosen to simulate these situations as closely as possible. Table II lists the tunnel conditions and parameter values examined.

TABLE I

Fumigation conditions: Great Lake area

Reference	Inversion top (m)	Wind ($\mathrm{m\ s^{-1}}$) velocity	Temperature sea surfaces (°C)	Temperature inland (°C)	Temperature upwind $z=L$ (°C)	L (m)	Ri_B	HR[a]
3 June 1966	~100	~5	10	27	19	100	1.51	1.89
12–13 August 1967	~500	5–6	12	24	21	100	1.45	1.33
25 June 1970	~500 (low level mixing depth) ~150	~6	11–13	16 (~8 km inland)	?	?	?	?
12–13 August 1973	?	5–6	?	?	?	?	?	?

[a] $L_z = 100$ m.

TABLE II

Wind-tunnel conditions for fumigation

$(V_a)_m$ ($m\ \mathrm{s^{-1}}$)	$(T_{\mathrm{water}})_m$ (°C)	$(T_H)_m$ (°C)	$(T_{\mathrm{land}})_m$ (°C)	Ri_B	HR[a]
0.6	0 ($z=0$) 4.5 ($z=4.5$ m)	38	127 ($z=0$) 54 ($z=4.5$)	1.0	1.5
0.6	0 ($z=0$) 4.5 ($z=4.5$ m)	38	93 ($z=0$) ($z=4.5$)	1.0	1.4
0.6	0 ($z=0$) 4.5 ($z=4.5$ m)	38	66 ($z=0$) ($z=4.5$)	1.0	1.35
1.2	0 ($z=0$) 4.5 ($z=4.5$ m)	38	127 ($z=0$) 54 ($z=4.5$)	0.25	1.5

[a] $(L_z)_m \simeq 0.3$ m.

3. Occurrence and Prediction of Plume Fumigation

Sea breezes or lake breezes are accompanied by turbulent transition-zone fumigations. The transition region begins at the shoreline and has the form of a wedge in which the turbulent air slopes upward with distance inland. At the point where the top of this wedge intersects an elevated plume, the contents of the plume will be mixed downward, becoming distributed between the plume and the ground. Van der Hoven (1967), Collins (1971), and Lyons and Olsson (1973) have examined dispersion near coasts. Observations of turbulent transition zones have been made at Big Rock Point Nuclear Plant (Hewson *et al.*, 1963) on Lake Michigan, Millstone Nuclear Power Station (Northeast Utilities, 1965) in Connecticut on Long Island Sound, and Humboldt Bay Power Plant (Pabman *et al.*, 1965) in California.

3.1. Plume behavior as emitted into stable atmosphere

While a smoke plume quickly attains the wind speed in the horizontal direction, its rise is determined by its vertical momentum and buoyancy. Numerous formulae have been published to correlate field measurements of plume rise; none is universally accepted, partially due to observational difficulties, and partially due to the fact that some plumes never really appear to level off.

The AEC-1968 monograph by Slade suggests the following expressions (Equations (5.19) and (5.20) rearranged in dimensionless form):

$$\text{Neutral} \quad \frac{\Delta h}{D_s} = 100\frac{\mathrm{R}}{\mathrm{Fr}} + 1.5R$$

$$\text{Stable with wind} \quad \frac{\Delta h}{D_s} = 1.63\left[\frac{RL^2}{\mathrm{Fr\ Ri}}\right]^{1/3}, \tag{1}$$

where

$$R = \frac{V_s}{V_a} \qquad \mathrm{Fr} \cong \frac{V_a^2}{g\dfrac{\Delta T}{T_s}D_s}$$

$$L = \frac{h_s}{D_s} \qquad \mathrm{Ri} = \frac{g\,(\mathrm{d}\theta/\mathrm{d}z)}{T_s(V_a^2/h_s^2)}.$$

Based on the work of Briggs (1969), one expects plume-rise predictions to be accurate within $\pm 19\%$. However, experience is very varied and some calculators have been conservative by a factor of five or optimistic by a factor of nearly two.

3.2. Mixing layer-plume interaction

When a plume initially emitted into a stable environment intercepts a mixing layer growing upward, 'fumigation' of the plume directly to the ground may occur. A number of authors have suggested means to estimate the magnitude of the ground

concentration resulting from such behavior. As summarized by Collins (1971), one method consists of determining the downwind distance at which a plume traveling horizontally at the effective stack height first intercepts the growing mixing layer. As a first approximation one may then assume that the maximum of the elevated plume concentrations at the downwind location now occurs at ground level.

Alternatively one may estimate the concentrations assuming a uniform vertical distribution throughout the layer of depth H:

$$\frac{\chi_{\max} V_a H^2}{Q} = \frac{1}{(2\pi)^{1/2}} \left(\frac{H}{\sigma_y}\right), \tag{2}$$

where from Figure A.2, Slade (1968), for stable flow (Pasquill stability Category F)

$$\frac{\sigma_y}{H} = 0.04 \left(\frac{x}{H}\right). \tag{3}$$

Lyons and Cole (1973) discuss a somewhat more complicated procedure which attempts to correct for rate of plume entrainment and rate of spreading in the mixing layer.

Van der Hoven (1967) has presented a graphical plot based on the report of Prophet (1961) for determining the depth of the mixing layer as a function of initial overwater stability and overland travel distance. An equation which fits his results is:

$$H = 8.8 \sqrt{\frac{x}{V_a \, \Delta\theta}}, \tag{4}$$

where

x (m) = distance overland
H (m) = height of mixed layer
V_a (m s^{-1}) = mean velocity
$\Delta\theta$ (°C) = overwater vertical difference in potential temperature within inversion layer.

Although differing in detail, simple theoretical and empirical formulations developed by Summers (1964) and Raynor *et al.* (1974) also display a one-half power dependence upon fetch, and reciprocal velocity and overwater temperature gradient. These expressions, however, require measurements of heat or momentum flux over the surfaces.

Dimensional analysis suggests that if the pertinent variables required to describe mixing-layer growth are

$$f(x, H, V_a, \Delta\theta, g, T, \Delta T, \delta) = 0, \tag{5}$$

where new variables listed are

T = absolute temperature
ΔT = land-water temperature difference
δ = characteristic height over which $\Delta\theta$ and V_a vary upstream.

Then appropriate dimensionless parameters might be

$$\frac{H}{\delta} = f\left(\frac{x}{\delta}, \frac{\Delta T}{\Delta\theta}, g\frac{\Delta\theta\delta}{TV_a^2}, \frac{V_a}{(g\delta)^{1/2}}\right) \tag{6}$$
$$= f\left(\frac{x}{\delta}, HR, \mathrm{Ri}_B, \mathrm{Fr}_\delta\right).$$

Examination of the mixing-layer growth results for this wind tunnel study reveals that initially $H \propto x^{0.8}$ followed by $H \propto x^{0.5}$. The initial region corresponds to behavior frequently observed for inner boundary-layer growth following a change of roughness. The subsequent region confirms the conclusions reached by Prophet. In addition it is found that $H \propto (HR)^6$. When these results are combined with Prophet's conclusion that $H \propto (V_a \Delta\theta)^{-1/2}$, it is found that

$$\frac{H}{\delta} = K\left(\frac{x}{\delta}\right)^{1/2} (HR)^6 (\mathrm{Ri}_B)^{-1/2} (\mathrm{Fr}_\delta)^{-3/2}. \tag{7}$$

When this result is compared to Equation (4) for $T \simeq 300°\mathrm{K}$, $\delta \simeq 100$ m, and $g = 9.86\ \mathrm{m\ s^{-2}}$, it is found that $K \simeq 0.01$. If the constant is based on measurements made herein, $K \simeq 0.015$.

Montgomery and Cain (1967) have compared the observed sulfur dioxide concentrations in the vicinity of a steam plant with those given by plume dispersion models. They concluded that general dispersion models cannot accurately predict specific pollutant concentrations at a particular station at a specific time, but they can predict the range of concentrations likely to occur. In addition, the same mathematical model using different diffusion coefficients may yield very different results, hence the diffusion coefficients should be developed for the model at the particular site of application (if possible).

4. Wind-Tunnel Experiment and Instrumentation

The use of a wind tunnel for model tests of gaseous diffusion by the atmosphere is based upon the concept that nondimensional concentration coefficients will be the same at contiguous points in the model and the prototype and will not be a function of the length-scale ratio. Concentration coefficients will only be independent of scale if certain similarity criteria are satisfied. These criteria are obtained by inspectional analysis of physical statements for conservation of mass, momentum and energy. Detailed discussions have been given by Halitsky (1963), Martin (1965), and Cermak *et al.* (1966). Basically the model laws may be divided into requirements for geometric, dynamic, thermic and kinematic similarity. In addition, similarity of upwind flow characteristics and surface boundary conditions must be achieved.

For this hypothetical power plant study, geometric similarity is satisfied by an un-

distorted model of length ratio 1:400. This scale was chosen to facilitate ease of measurements, provide a boundary layer equivalent to 240–300 m for the atmosphere and minimize wind-tunnel blockage. (The ratio of projected area to the area of the wind-tunnel cross-section should not exceed 5%. The model of the power plant at a scale of 1:400 produced a blockage of 2.7%.)

To summarize, the following scaling criteria were applied:

(1) $\mathrm{Re}=\varrho_a V_a L_z/\mu_a > 11000$,
(2) $\mathrm{Fr}=\varrho_a V_a/\Delta\gamma\, D_s$; $(\mathrm{Fr})_m=(\mathrm{Fr})_p$,
(3) $R=Vs/V_a^2$; $R_m=R_p$,
(4) $(z_0)_m=(z_0)_p$,
(5) Similar velocity and turbulence profiles upwind,
(6) $HR=1.3\sim1.9$,
(7) $\mathrm{Ri}_B=1.25\sim1.5$.

It has been found that other turbulence scales such as intensities and spectral shapes will generally be reproduced satisfactorily if the fourth and fifth conditions are maintained over a sufficiently long fetch (Cermak *et al.*, 1966).

4.1. Wind tunnel

The meteorological wind tunnel (MWT) in the Fluid Dynamics and Diffusion Laboratory, Colorado State University was used for the study. This wind tunnel, especially designed to study atmospheric flow phenomena, incorporates special features such as adjustable ceiling, rotating turntable, temperature controlled boundary wall, and long test section to permit adequate reproduction of micrometeorological behavior. Mean wind speeds of 0.06 to 40 m s^{-1} (0.14 to 90 mph) in the MWT can be obtained. Boundary-layer thickness up to 1.2 m can be developed over the downstream 6 m of the MWT test section. Thermal stratification in the MWT is provided by the heating and cooling systems in the section passage and the test section floor. The flexible test section roof on the MWT is adjustable in height to permit the longitudinal pressure gradient to be set at zero.

4.2. Test configuration in the MWT

Only two wind approach angles were examined for the fumigation study – onshore and 60° to the shoreline. A set of vortex generators were installed 0.6 m downwind of the entrance to give the simulated boundary an initial impulse of growth. Between 1.8 and 12 m downstream, a set of 12 roll-bond aluminum panels were placed on the tunnel floor. These panels were connected to the facility refrigeration system and cooled to approximately 0 °C. Fillets were installed in the bottom tunnel corners to cover the plumbing connections and reduce resulting wake turbulence. From 12 m to the end of the test section, a permanently installed set of electric heaters was used to raise the aluminum floor temperature to a level prescribed by the heating ratio, *HR*. An array of ground-level sampling tubes permitted concentration measurements downwind to an equivalent field distance of 2400 m (see Figure 1).

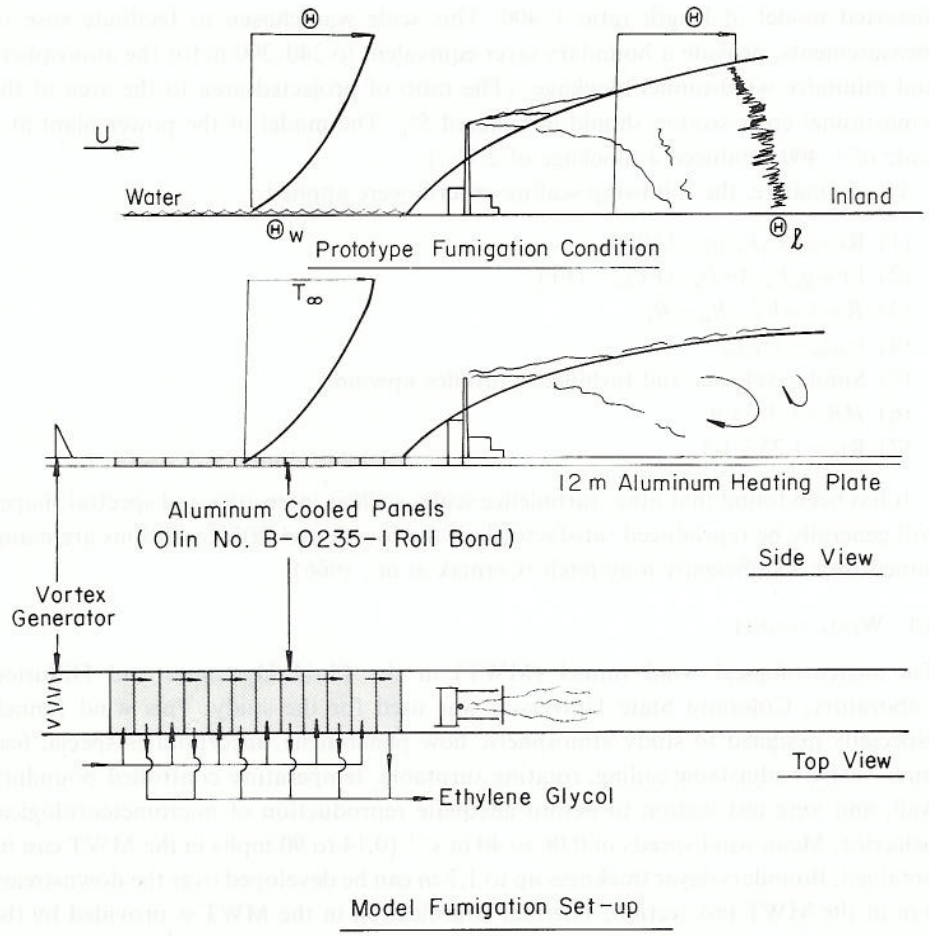

Fig. 1. Schematic diagram of model study of fumigation dispersion.

The model consisted of the power station, the stacks, and the auxiliary buildings constructed from aluminum to a linear scale of 1:400 (see Figure 2). A basic flat topography was reproduced by fixing the model to a 0.6 cm thick aluminum plate. Aluminum was chosen to allow model heating during the onshore-breeze fumigation study phase.

Metered quantities of gas were allowed to flow from each stack to simulate the exit velocity and also account for buoyancy effects due to the temperature difference between the stack gas and the ambient atmosphere. Helium and compressed air were mixed in metered amounts to adjust the specific weight. Flow settings were adjusted for pressure, temperature, and molecular weight effects as necessary. When a visible plume was required, the gas was bubbled through titanium tetrachloride before emission. When a traceable plume was required, a high pressure mixture of Krypton-85 and air was used in place of the compressed air.

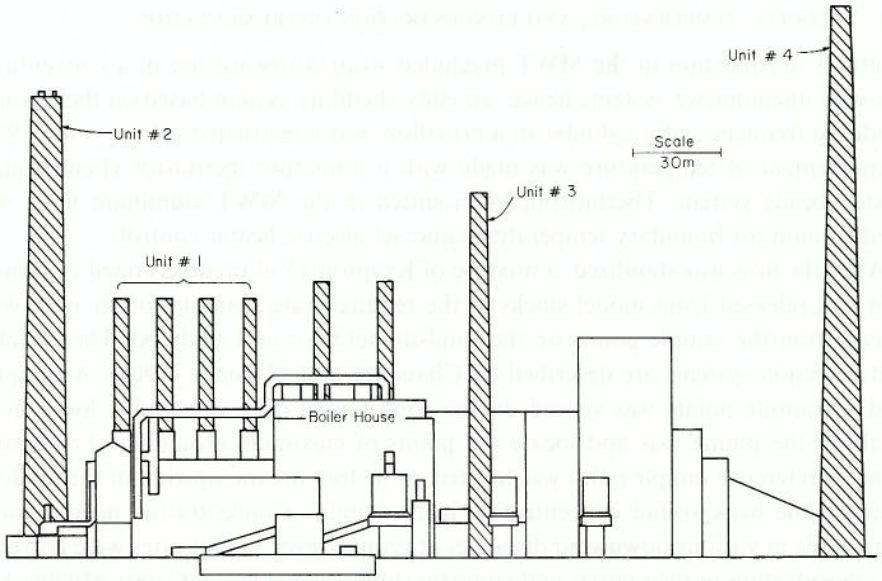

Fig. 2. Power Plant, looking landward.

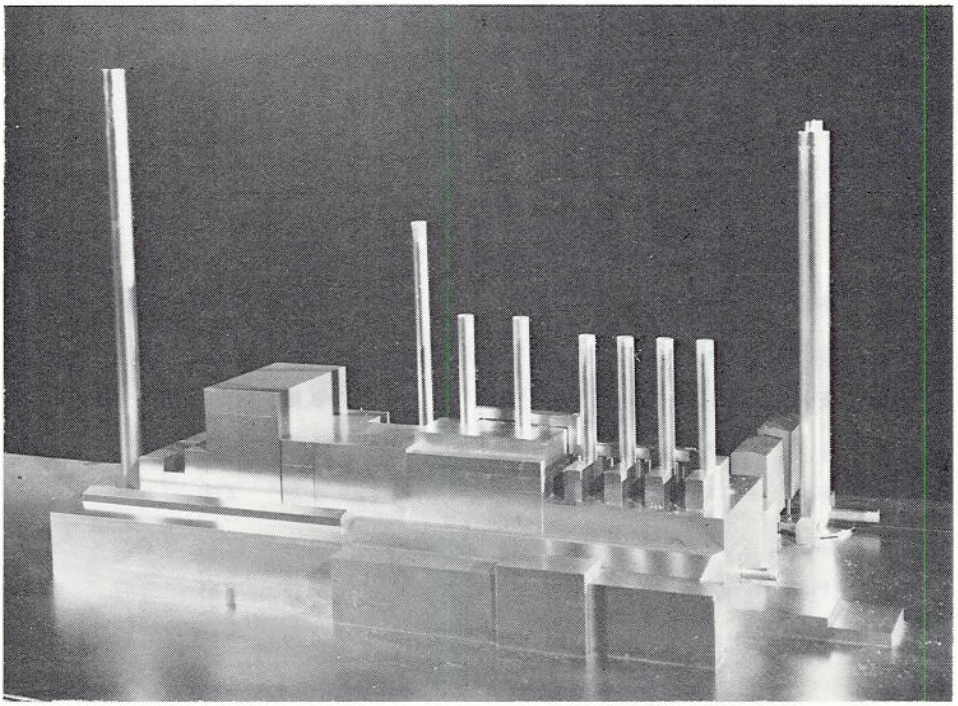

Fig. 2b. Picture of the model of hypothetical shore-line Power Plant.

4.3. Velocity, temperature, and concentration instrumentation

Thermal stratification in the MWT precluded straightforward use of a conventional hot-wire anemometer system; hence, an eddy shedding system based on the Strouhol shedding frequency of a cylinder in a crossflow was constructed (Hoot *et al.*, 1973). Measurement of temperature was made with a miniature thermistor (Fennel glass-coated bead) system. Thermocouples mounted in the MWT aluminum floor were used to monitor boundary temperatures and set electric heater controls.

After the flow was stabilized, a mixture of Krypton-85 of predetermined concentration was released from model stacks at the required rate. Samples of air were withdrawn from the sample points on the wind-tunnel floor and analyzed. The sampling and detection systems are described by Chaudhry and Meroney (1969). A sampling grid of sample points was spaced on the wind-tunnel floor at suitable locations to establish the plume axis and locate the points of maximum ground-level concentrations. A reference sample point was located in the free stream, upwind of the model to measure the background concentration in the tunnel. Concentration measurements were made at various downwind distances at ground level. Count rates were corrected to concentration in pico-curies and compensation was made for Geiger Mueller tube dead time. Final results are reported in terms of $V_a\chi/Q$ which has dimensions of inverse length squared.

Interpretation of wind-tunnel concentrations in terms of an equivalent field averaging time remains somewhat vague. In the absence of buildings, heating or rough terrain, experience suggests an equivalent prototype averaging time of from 2 to 10 min. However, in the presence of the above factors, it may be more appropriate to be

TABLE III

Stack emission parameters

Units	Load	Stack velocity ($m\ s^{-1}$)	Stack diam (m)	Stack height (m)	Stack gas temp (°C)	V_a=6.7 $m\ s^{-1}$ R	Fr	V_a=13.4 $m\ s^{-1}$ R	Fr
1	Full	5.2	17	116	195	0.77	4.08	0.38	16.32
(4 stacks)	$\frac{1}{3}$	1.6			183	.24	5.21	0.12	20.84
2	Full	21.3	3.7[a]	150 or 180	199	3.18	5.36	1.59	21.46
	$\frac{1}{3}$	7.5			184	1.11	7.16	0.56	28.64
3	Full	11.9	5.1	120	198	1.77	4.00	0.88	15.84
	$\frac{1}{3}$	3.7			184	0.55	5.15	0.28	20.62
4	Full	18.9	7.3	180	202	2.83	2.61	1.42	10.46
	$\frac{1}{3}$	6.0			188	0.89	3.28	0.46	13.11

Note: V_{ap} V_{am}

6.7 $m\ s^{-1}$ (15 mph) 0.6 $m\ s^{-1}$

13.4 $m\ s^{-1}$ (30 mph) 1.2 $m\ s^{-1}$

[a] Unit 2 has two 3.7-m flues on top.

conservative and use 20–30 min as a comparative value. Velocity V_a and temperature T may be considered to have similar time average significance.

5. Results and Discussion

The test program consisted of: (1) a qualitative study of the flow field around the power plant by visual observation of the smoke plume trajectory from the stacks; and (2) a quantitative study of gas concentrations produced by the release of Krypton-85 from the stacks. The test conditions are summarized in Tables II and III.

5.1. Test results: characteristics of flow

All experiments were carried out in the MWT over the range of conditions shown in Table II. The atmospheric boundary layer was modeled to produce a velocity and temperature profile equivalent to flow over an open lake. Figure 3 shows the initial

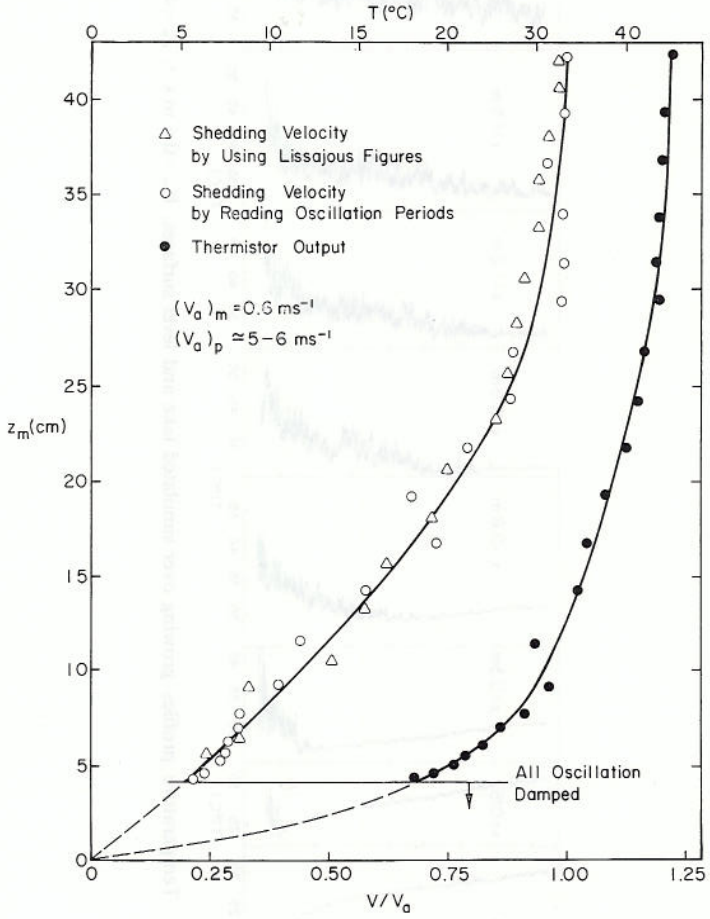

Fig. 3. Upwind mean velocity and temperature profiles: fumigation condition.

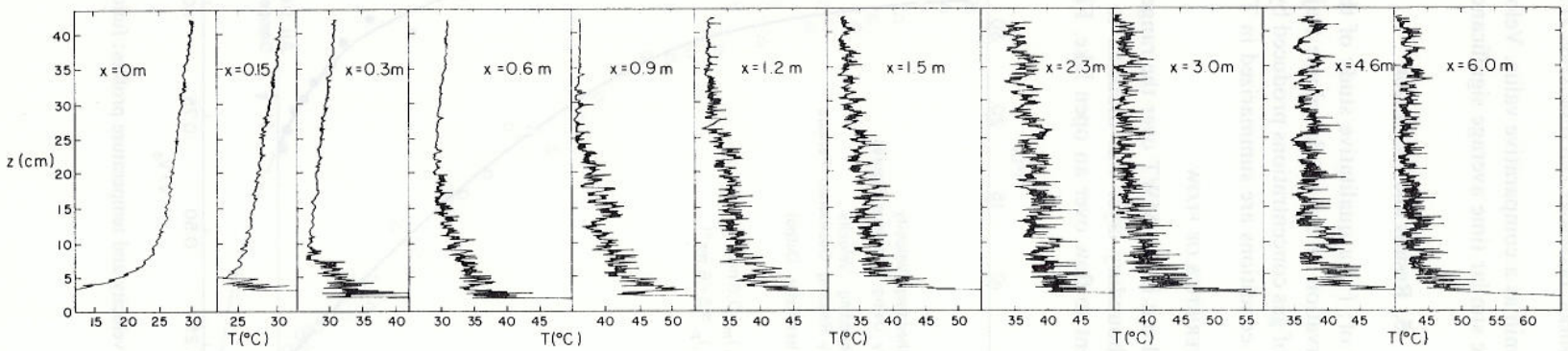

Fig. 4. Temperature profiles growing over simulated lake and level surfaces, $V_m = 0.6$ m s^{-1}, $T_a = 43$°C, T_w upwind $= 0$°C, T_w downstream $= 127$°C.

upwind profiles of velocity and temperature. Turbulence was essentially absent as evidenced by the behavior of smoke plumes released over the cooled model lake surface. The profiles are conditioned by the heated land surface and the presence of the building complex. Turbulent well-mixed surface flow grows beneath the capping stable lake air. Figure 4 displays the eroding effect of unstable air. The small thermistor temperature measuring device had a short time constant; thus the temperature fluctuations displayed are an indicator of the intensity of turbulence.

Intensity and power spectral estimates of the various components of turbulence have not yet been successfully obtained for the low laboratory speeds required for simulation.

Figure 5 displays the boundary-layer growth for the three surface heating intensities studied. Initially the region grows at a rate proportional to downwind distance to the 0.8 power. Subsequently beyond about 300 to 600 scaled metres, the growth rate is proportional to downwind distance to the 0.5 power. The behavior of the initial region corresponds to previous experience over slightly roughened surfaces. The later growth rate corresponds to behavior noted by Prophet (1961) for sea- and lake-breeze systems and by Deardorff *et al.* (1969) for a laboratory study with penetrative convection of buoyant elements.

Ogawa (1973) reports an exploratory study of the lower sea-breeze layer in a wind tunnel at New York University. The reported experiments had a maximum $HR \cong 1.35$ and an upstream $Ri_B \simeq 0.1$. These are rather low compared to the prototype situation. The height of the inversion base was reported to increase linearly with distance. It is

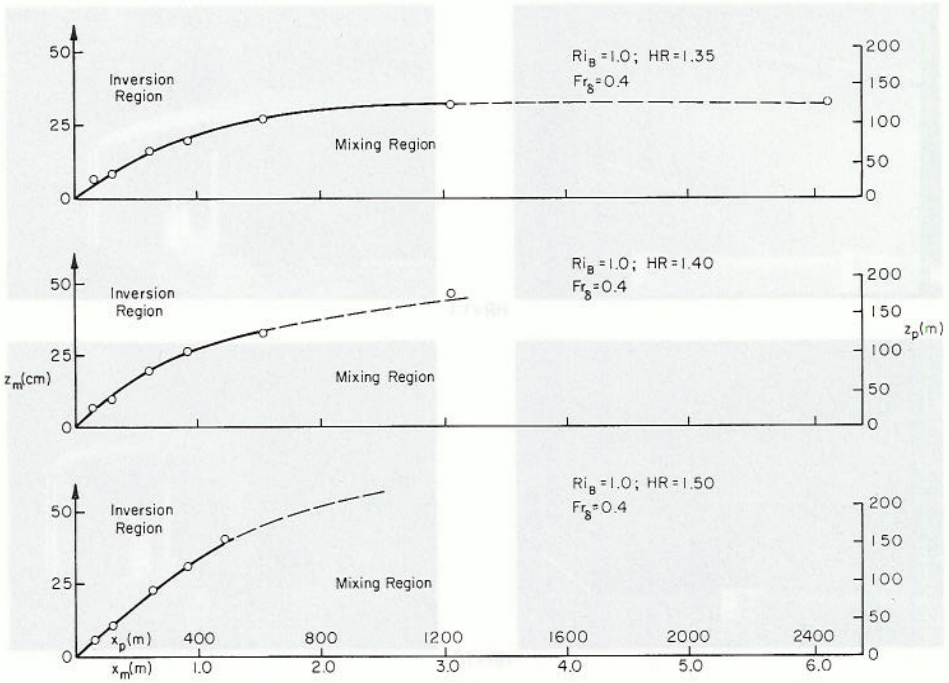

Fig. 5. Growth of the mixing layer at various floor temperatures.

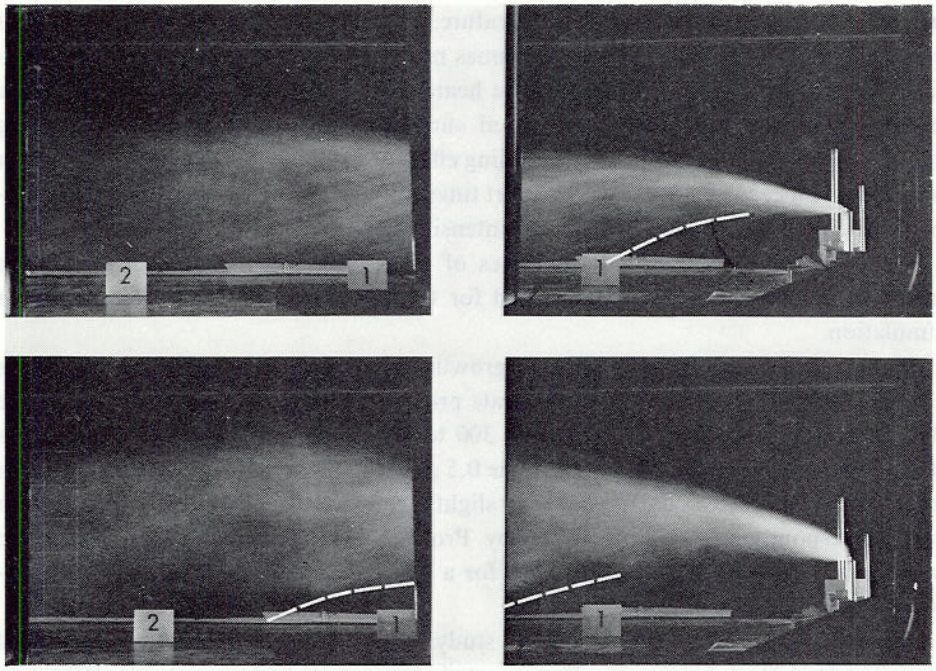

Fig. 6. Flow visualization, fumigation, unit 1, wind angle onshore wind speed 6.7 m s^{-1}, load full and one-third, $HR=1.5$.

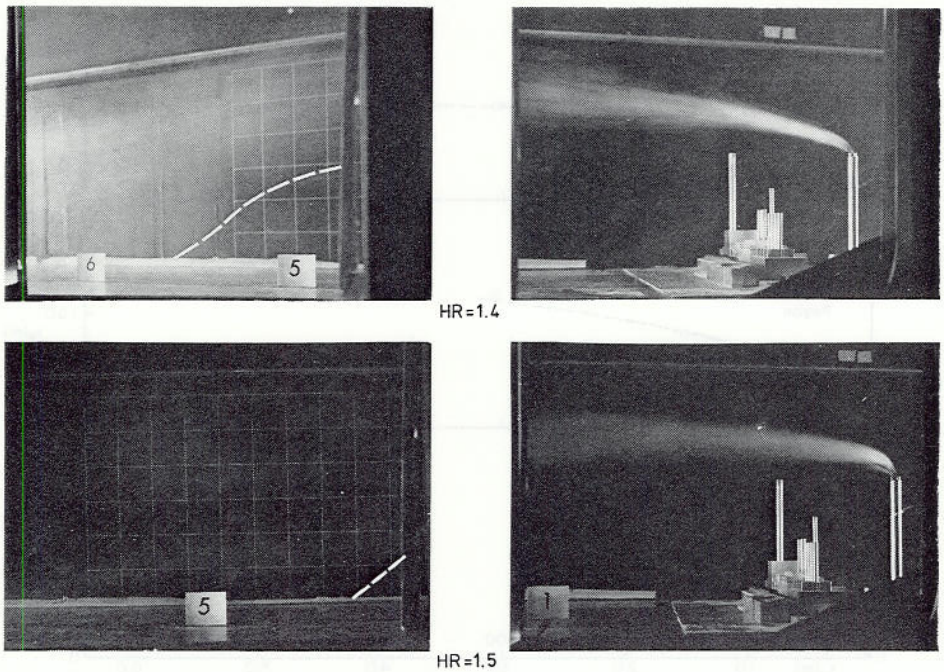

Fig. 7. Flow visualization, fumigation, unit 2 full load, wind angle onshore, wind speed 6.7 m s^{-1}, $HR=1.5$, 1.4.

probable that heating was not intense enough, and/or that the test section was not long enough.

Ogawa found that dispersion beneath the inversion base was at a rate comparable with dispersion in a fully unstable region. Vertical mixing of course is initially limited by the inversion base; downstream, however, the plume did not appear to differ in behavior from one emitted into a fully unstable region.

When the model is in place, the building complex wake displaces the inner boundary layer upwards significantly. Thus the maximum ground-level concentration occurs closer to the plant site than if all emissions were from an isolated stack.

5.2. Test results: visualization

The test results consist of photographs and movie sequences showing the nature of the air flow and diffusion in the vicinity of the power station. The sequence of photographs shown in Figures 6 and 7 shows side views of the behavior of a smoke plume released from a stack for a direct onshore wind for full load at various land surface heating rates. The more intense heating ($HR = 1.5$) accelerates the mixed-layer growth and the entrainment of the plume. A decrease in hypothetical load from full to one-third has the same effect on the initial plume as does an increase in wind speed; however, the character of the surface mixed layer remains the same.

The observed 'touchdown' distances evaluated from the flow visualization tests are summarized in Tables IV and V. These distances represent locations where, by visual inspection, the plume resides greater than 10% of the time. Once the plume intercepts the inner boundary layer, the smoke is mixed downward at a rate which gives a lower plume boundary angle of about 30 to 45°. Hence the plume is not brought immediately to the surface after it enters the mixing layer as suggested by the simplified physical model.

TABLE IV

Test results: neutral

Units	Nominal wind direction	Velocity ($m\ s^{-1}$)	Full load			$\frac{1}{3}$ Load		
			Touch-down distance	Maximum ground concentration		Touch down distance	Maximum ground concentration	
				Distance	Magnitude		Distance	Magnitude
			(m)	(m)	(m^{-2})	(m)	(m)	(m^{-2})
	−30°	6.7	450	2400	0.237×10^{-5}	300	1800	0.350×10^{-5}
1		13.4	150	1200	0.123×10^{-4}	400	600	0.316×10^{-4}
2	0°	6.7	>2400	–	–	1800	–	–
(150 m		13.4	1400	–	–	600	–	–
stack)	−30°	6.7	>2400	2100	0.755×10^{-6}	760	–	–
		13.4	550	2400	0.141×10^{-4}	550	2100	0.102×10^{-4}
3	−30°	6.7	900	–	–	450	–	–
		13.4	400	1200	0.159×10^{-4}	450	1200	0.287×10^{-4}
4	−30°	6.7	>2400	–	–	1200	–	–
		13.4	1800	1800	0.143×10^{-5}	1400	1800	0.813×10^{-5}

TABLE V

Test results: model sea breeze

Units	Nominal wind direction	Velocity ($m\ s^{-1}$)	Heating rate	Full Load			$\frac{1}{3}$ Load		
				Touchdown distance	Maximum ground concentration		Touchdown distance	Maximum ground concentration	
					Distance[a]	Magnitude[b]		Distance	Magnitude
				(m)	(m)	(m^{-2})	(m)	(m)	(m^{-2})
	0°	6.7	1.5	450	–	–	300	–	–
1	−30°	6.7	1.5	300	1500	0.365×10^{-5}	450	900	0.474×10^{-5}
2	0°	6.7	1.5	1200	1800	0.695×10^{-5}	600	1200	0.335×10^{-4}
(h_s=150 m)			1.4	1700	–	–	900	-	–
		13.4	1.5	1500	–	–	900	–	-
	−30°	6.7	1.5	1200	1800	0.265×10^{-4}	750	1200	0.380×10^{-4}
			1.4	1500	2400	0.135×10^{-4}	900	1500	0.238×10^{-4}
			1.35	–	2400	0.221×10^{-5}	–	1800	0.226×10^{-4}
		13.4	1.5	1400	–	–	900	–	–
2	0°	6.7	1.5	1400	–	–	1000	–	–
(h_s=180 m)			1.4	2000	–	–	900	–	–
		13.4	1.5	2100	2400	0.565×10^{-5}	1200	1800	0.238×10^{-4}
	−30°	6.7	1.5	1400	2400	0.964×10^{-5}	750	1200	0.337×10^{-4}
			1.4	1500	2400	0.155×10^{-5}	900	2400	0.174×10^{-4}
			1.35	–	–	–	–	1800	0.133×10^{-4}
		13.4	1.5	1700	–	–	750	–	–
3	0°	6.7	1.5	900	–	–	400	–	–
	−30°	6.7	1.5	700	1200	0.659×10^{-5}	400	600	0.329×10^{-4}
4	0°	6.7	1.5	1800	–	–	900	–	–
		13.4	1.5	1200	–	–	900	–	–
	−30°	6.7	1.5	2000	2400	0.128×10^{-4}	975	1500	0.345×10^{-4}

[a] Distance to Mamimum Ground Concentration

[b] $\chi V/Q$

5.3. Test results: concentration measurements

Twenty-five ground-level sampling locations were placed at distances equivalent to 300 to 2400 m downwind. Measurements of Krypton-85 activity at these locations have been converted to equivalent $\chi V_a/Q$ (m^{-2}). Typical results for various sources, loads, wind angles, wind velocities, and surface heating rates are presented in Figures 8 and 9. The maximum measured concentration and its respective downwind location for each situation are also given in Tables IV and V. For full load, Unit 2 maximum concentrations occurred for a 150-m stack at $-30°$ – i.e., 0.265×10^{-4} (m^{-2}). A 180-m stack provided enough additional plume elevation to reduce this to one-third the level – i.e., 0.964×10^{-5} (m^{-2}). For a one-third load situation the 150 and 180 m stacks develop ground-level concentrations of 0.380×10^{-4} and 0.337×10^{-4} (m^{-2}), respectively.

It is, of course, instructive to compare the measurements discussed here with the results of calculations based on Section 3. Consider a test stack at full load, Unit 2:

	R	Fr	Ri_B	Fr_δ	V_a (ms^{-1})	$h_s+\Delta h$ (m)	$V_a\chi/Q$ (m^{-2})
Neutral	3.18	5.36	0.0	–	6.7	234	0.357×10^{-7}
Stable (Fumigation)	3.18	5.36	1.0	0.39	6.7	212	0.785×10^{-5}

This may be compared with a maximum concentration from the model study of 0.755×10^{-6} (m^{-2}) for the comparable neutral case and 0.265×10^{-4} (m^{-2}) for the

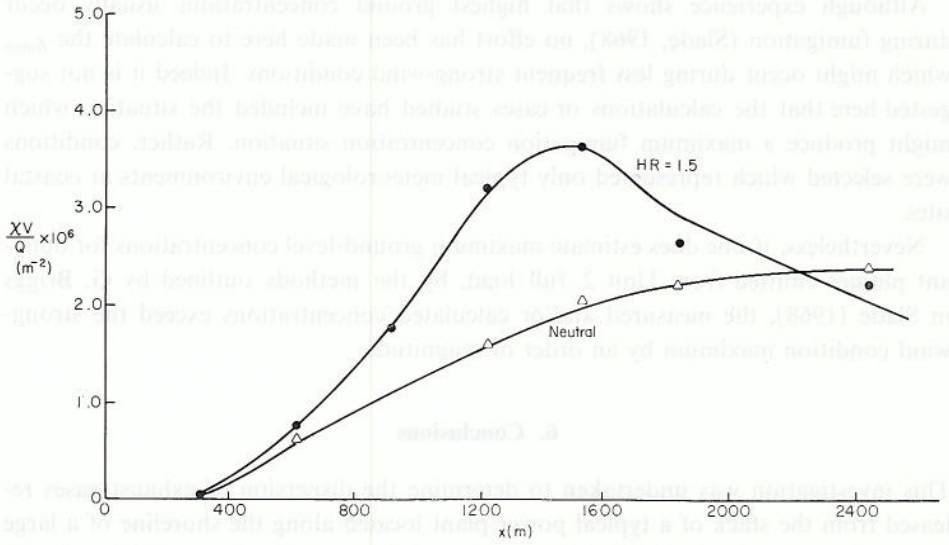

Fig. 8. Ground-level concentrations Unit 1, Full load, Angle = 30°, Neutral vs Model Sea Breeze, $V_a \simeq 6.7$ m s^{-1}.

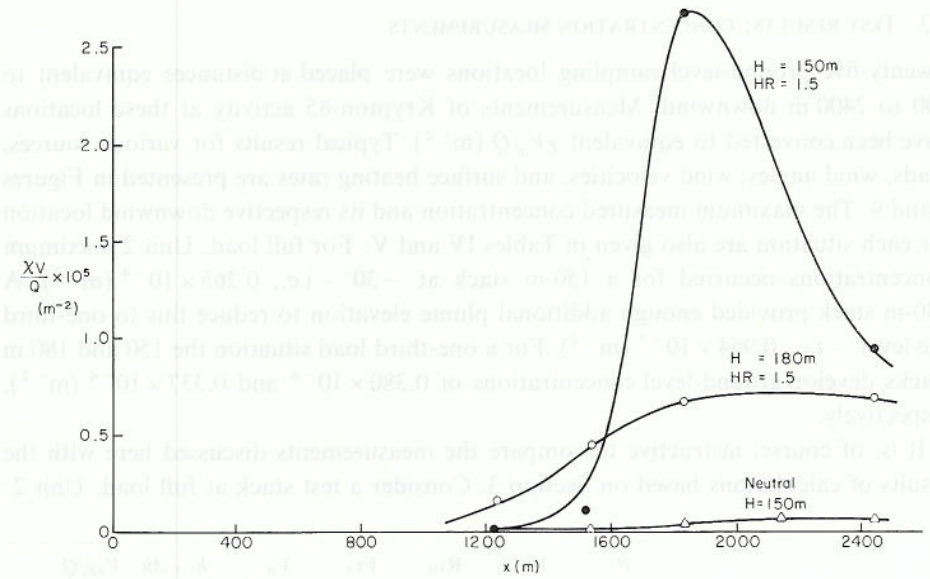

Fig. 9. Ground-level concentrations Unit 2, Full load, Angle = −30°, Neutral vs Model Sea Breeze, $V_a = 6.7$ m s^{-1}.

comparable fumigation case. In each case the increased concentration may be attributed to the accelerated mixing due to the aerodynamic turbulence generated by the building complex. On the other hand, the differences may be largely due to shortcomings in the extremely simple analytical models used.

Although experience shows that highest ground concentrations usually occur during fumigation (Slade, 1968), no effort has been made here to calculate the χ_{max} which might occur during less frequent strong-wind conditions. Indeed it is not suggested here that the calculations or cases studied have included the situation which might produce a maximum fumigation concentration situation. Rather, conditions were selected which represented only typical meteorological environments at coastal sites.

Nevertheless, if one does estimate maximum ground-level concentrations for buoyant plumes emitted from Unit 2, full load, by the methods outlined by G. Briggs in Slade (1968), the measured and/or calculated concentrations exceed the strong-wind condition maximum by an order of magnitude.

6. Conclusions

This investigation was undertaken to determine the dispersion of exhaust gases released from the stack of a typical power plant located along the shoreline of a large lake or the ocean. On the basis of the experimental measurements reported herein, the following comments may be made:

(1) Plumes from all stacks are entrained into the surface mixed layer as it grows over the land. This results in greater ground-level concentrations than found in the equivalent neutral situation. The result is most severe for plumes released from the shorter stacks.

(2) The highest ground-level concentration for any stack during the stratified condition is three times greater than that occurring during the worst neutral flow situation.

(3) For taller isolated stacks, such as Unit 2 (Figure 9), vertical mixing may increase ground-level concentrations to six times those occurring during the worst neutral condition. This statement must be tempered by the fact that the neutral maximum is itself not very large.

(4) Increasing the stack height for tall stacks such as Units 2 from 150 to 180 m may reduce the ground concentration maximum by only one-third.

(5) Earlier mixing-layer equations based on the results of Prophet (1971) do not appear adequate to predict behavior over the Great Lakes (Lyons and Cole, 1973), or in this laboratory investigation. Prophet's results are suspect since they do not include the influence of land-sea temperature difference.

References

Barrett, R. V.: 1973, 'Use of the Wind Tunnel to Investigate the Influence of Topographical Features on Pollution from a Tall Stack', Chimney Design Symposium, April 9–11, Edinburgh, Scotland, 16 pp.

Briggs, G. A.: 1969, 'Plume Rise', U.S. Atomic Energy Commission (Available as TID-25075), 81 pp.

Cermak, J. E.: 1971, 'Laboratory Simulation of the Atmospheric Boundary Layer', *Amer. Inst. Aeron. Astron. J.* **9**, 1746–1754.

Cermak, J. E., Sandborn, V. A., Plate, E. J., Binder, G. J., Chuang, H., Meroney, R. N., and Ito, S.: 1966, 'Simulation of Atmospheric Motion by Wind-Tunnel Flows', Colorado State University, Report Number CER66-JEC-VAS-EJP-GJB-HC-RNM-SI-17.

Chaudhry, F. and Meroney, R. N.: 1969, 'Turbulent Diffusion in a Stably Stratified Shear Layer', U.S. Army Electronic Command Report C-0423-5 Contract DAAB07-68-C-0423, FDDL Report CER69-70-FHC-RNM12, Colorado State University.

Collins, G. F.: 1971, 'Predicting Sea Breeze Fumigation from Tall Stacks at Coastal Locations', *Nucl. Safety* **12**, 110–114.

Deardorff, J. W., Willis, G. E., and Lilly, D. K.: 1969, 'Laboratory Investigation of Non-Steady Penetrative Convection', *J. Fluid Mech.* **35**, 7–31.

Fisher, D. C.: 1960, 'An Observational Study of the Sea Breeze', *J. Meteorol.* **17**, 645–660.

Fisher, E. C.: 1961, 'A Theoretical Study of the Sea Breeze', *J. Meteorol.* **18**, 216–233.

Halitsky, J.: 1963, 'Gas Diffusion Near Buildings', *Geophysical Science Laboratory Report No. 63-3*, New York University.

Haurwitz, B.: 1947, 'Comments on the Sea-Breeze Circulation', *J. Meteorol.* **4**, 1–8.

Hess, S. L.: 1959, *Introduction to Theoretical Meteorology*, Holt, Rinehart and Winston, New York, 362 pp.

Hewson, E. W., Gill, G. C., and Walker, G. J.: 1963, 'Smoke Plume Photography Study, Big Rock Paint Nuclear Power Plant, Charlevoix, Michigan', University of Michigan, Dept. of Meteorology and Oceanography, Ann Arbor, Michigan.

Hoot, T. G., Meroney, R. N., and Perterka, J. A.: 1973, 'Wind Tunnel Tests of Negatively Buoyant Plumes', FDDC Report CGR73-74TGH-RNM-JAP13, Colorado State University.

Humphreys, W. J.: 1964, *Physics of the Air*, Dover, 676 pp.

Lyons, W. A.: 1970, 'Mesoscale Transport of Pollutants in the Chicago Area as Affected by Land and Lake Breezes', Proceedings 2nd International Clean Air Congress, Washington, D.C., pp. 973–978.

Lyons, W. A. and Cole, H. S.: 1971, 'Fumigation and Plume Trapping: Aspects of Mesoscale

Dispersion on the Shores of Lake Michigan in Summer During Records of Stable Onshore Flow', Conference on Air Pollution Meteorology, Raleigh, North Carolina, April 5–9, p. 42–47.

Lyons, W. A. and Cole, H. S.: 1973, 'Fumigation and Plume Trapping on the Shores of Lake Michigan During Stable Onshore Flow', *J. Appl. Meteorol.* **12**, 494–510.

Lyons, W. A. and Olsson, L. E.: 1973, 'Detailed Mesometeorological Studies of Air Pollution Dispersion in the Chicago Lake Breeze', *Monthly Weather Rev.* **101**, 387–403.

Martin, J. E.: 1965, 'The Correlation of Wind Tunnel and Field Measurements of Gas Diffusion Using KR-85 as a Tracer', Ph.D. Dissertation, MMPP 272, University of Michigan.

Montgomery, T. L. and Cain, M.: 1967, 'Adherence of Sulfur Dioxide Concentrations in the Vicinity of a Steam Plant to Plume Dispersion Models', *J. Air Pollution Control Assoc.* **17**, 512–517.

Moroz, W. J.: 1967, 'A Lake Breeze on the Eastern Shore of Lake Michigan; Observation and Model', *J. Atmospheric Sci.* **24**, 337–355.

Northeast Utilities: 1965, 'Millstone Nuclear Power Station, Waterford, Connecticut, Design and Analysis Report', Vol. I, USAEC Rocket No. 50245, U.S. Atomic Energy Commission, Directorate of Licensing, Washington, D.C.

Ogawa, Y.: 1973, 'Effects of Building and Thermal Boundary Layer in Diffusion', Ph. D. Dissertation, Faculty of Engineering, Hokkaido University, Sapporo, Japan, 327 pp.

Olfe, D. B. and Lee, R. L.: 1971a, 'Linearized Calculations of Urban Heat Island Convection Effects', AIAA Paper No. 71-13, AIAA 9th Aerospace Sciences Meeting, New York, New York, 14 pp.

Olfe, P. B. and Lee, R. L.: 1971b, 'Linearized Calculations of Urban Heat Island Convection Effects', *J. Atmospheric Sci.* **38**, 1374–1388.

Pabman, L. H., Eberly, D. L., and Cramer, H. E.: 1965, 'Meteorology and Atmospheric Diffusion in the Vicinity of the Humboldt Bay Power Plant', Pacific Gas and Electric Co., Meteorological Office, San Francisco, California.

Prophet, D. T.: 1961, 'Survey of the Available Information Pertaining to the Transport and Diffusion of Airborne Material Over Ocean and Shoreline Complexes', Technical Report 89(AD-258958), Aerosol Laboratory, Stanford University.

Raynor, G. S., Michael, P., Brown, R. M., and SethuRaman, S.: 'A Research Program on Atmospheric Diffusion From an Oceanic Site', AMS Symposium on Atmospheric Diffusion and Air Pollution, Sept. 9–13 1974, Santa Barbara, California, pp. 289–295.

SethuRaman, S. S. and Cermak, J. E.: 1973, 'Physical Modeling of Flow and Diffusion Over an Urban Heat Island', Proc. 2nd IUTAM-IUGG Symposium on Turbulent Diffusion in Environmental Pollution, Charlottesville, Virginia, 8–14 April.

Slade, D. H.: editor: 1968, 'Meteorology and Atomic Energy-1968', U.S. Atomic Energy Commission, TID-24190.

Summers, P. W.: 1964, 'An Urban Ventilation Model Applied to Montreal', Ph.D Dissertation, Dept. of Meteorology, McGill University, Montreal, Canada.

Van der Hoven, I.: 1967, 'Atmospheric Transport and Diffusion at Coastal Sites', *Nucl. Safety* **8**, 490–499.

Wexler, R.: 1946, 'Theory and Observation of Land and Sea Breezes', *Bull. Am. Meteorol. Soc.* **27**, 272–287.

Yamada, T. and R. N. Meroney: 1971, 'Numerical and Wind Tunnel Simulation of Response of Stratifies Shear Layers to Nonhomogeneous Surface Features', Project Themis Tech. Report No.9, ONE Contract No. N00014-68-A-0493-0001, FDPL Report No. CER70-71TY-RNM62.